Journal of Medicinal Chemistry

Article

pubs.acs.org/jmc

Discovery of a Novel, First-in-Class, Orally Bioavailable Azaindole Inhibitor (VX-787) of Influenza PB2

Michael P. Clark,*[,†] Mark W. Ledeboer,[†] Ioana Davies,[†] Randal A. Byrn,[†] Steven M. Jones,[†] Emanuele Perola,[†] Alice Tsai,[†] Marc Jacobs,[†] Kwame Nti-Addae,[†] Upul K. Bandarage,[†] Michael J. Boyd,[†] Randy S. Bethiel,[†] John J. Court,[†] Hongbo Deng,[†] John P. Duffy,[†] Warren A. Dorsch,[†] Luc J. Farmer,[‡] Huai Gao,[†] Wenxin Gu,[†] Katrina Jackson,[†] Dylan H. Jacobs,[†] Joseph M. Kennedy,[†] Brian Ledford,[†] Jianglin Liang,[†] François Maltais,[†] Mark Murcko,[†] Tiansheng Wang,[†] M. Woods Wannamaker,[†] Hamilton B. Bennett,[†] Joshua R. Leeman,[†] Colleen McNeil,[†] William P. Taylor,[†] Christine Memmott,[†] Min Jiang,[†] Rene Rijnbrand,[†] Christopher Bral,[§] Ursula Germann,[†] Azin Nezami,[†] Yuegang Zhang,[†] Francesco G. Salituro,[∥] Youssef L. Bennani,[‡] and Paul S. Charifson[†]

[†]Vertex Pharmaceuticals Inc., 50 Northern Ave, Boston, Massachusetts 02210, United States

[‡]Vertex Pharmaceuticals (Canada) Inc., 275 Armand-Frappier, Laval, Quebec H7V 4A7, Canada

[§]Arrowhead Research Corporation, 465 Science Drive, Suite C, Madison, Wisconsin 53711, United States

[∥]Sage Therapeutics, 215 First Street, Cambridge, Massachusetts 02141, United States

Supporting Information

ABSTRACT: In our effort to develop agents for the treatment of influenza, a phenotypic screening approach utilizing a cell protection assay identified a series of azaindole based inhibitors of the cap-snatching function of the PB2 subunit of the influenza A viral polymerase complex. Using a bDNA viral replication assay (Wagaman, P. C.; Leong, M. A.; Simmen, K. A. Development of a novel influenza A antiviral assay. *J. Virol. Methods* **2002**, *105*, 105−114) in cells as a direct measure of antiviral activity, we discovered a set of cyclohexyl carboxylic acid analogues, highlighted by VX-787 (**2**). Compound **2** shows strong potency versus multiple influenza A strains, including pandemic 2009 H1N1 and avian H5N1 flu strains, and shows an efficacy profile in a mouse influenza model even when treatment was administered 48 h after infection. Compound **2** represents a first-in-class, orally bioavailable, novel compound that offers potential for the treatment of both pandemic and seasonal influenza and has a distinct advantage over the current standard of care treatments including potency, efficacy, and extended treatment window.

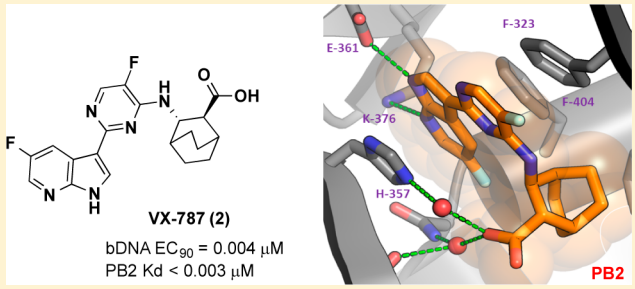

INTRODUCTION

The orthomyxoviridae family of RNA viruses includes influenza A, B, and C. Influenza is responsible for more than 200 000 hospitalizations[2] on a yearly basis and an annual mortality rate that varies from 3000 to 49 000 deaths in the United States during nonpandemic seasons.[3] Both swine and avian hosts can serve as reservoirs of influenza A. Occasionally, transmission of a new flu variant from other species to humans can lead to a global epidemic, such as the 2009 H1N1 swine flu pandemic. The emergence of the highly pathogenic H5N1 and H7N9 avian influenza strains emphasizes the continued potential global risk of the jumping of animal influenza strains to the human population.[4] The current standard of care (SOC) antivirals for influenza cases in the United States are the neuraminidase inhibitors (NAIs) oseltamivir (**1**, Figure 1) and zanamivir. While these agents can be effective against a variety of type A and B influenza viruses, they suffer from two main limitations. First, the neuraminidase inhibitors have only a moderate impact on the severity of symptoms as well as duration of sickness and they must be administered within 24−48 h of infection.[5] Second, resistance to this class of antivirals

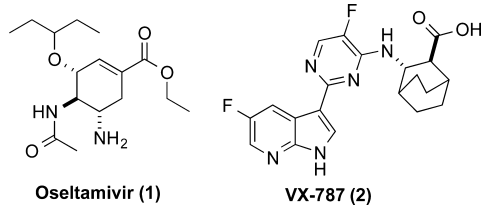

Figure 1. Inhibitors of influenza virus: NA inhibitor oseltamivir (**1**) and **2**.

Received: May 9, 2014
Published: July 14, 2014

   dx.doi.org/10.1021/jm5007275 | *J. Med. Chem.* 2014, 57, 6668−6678

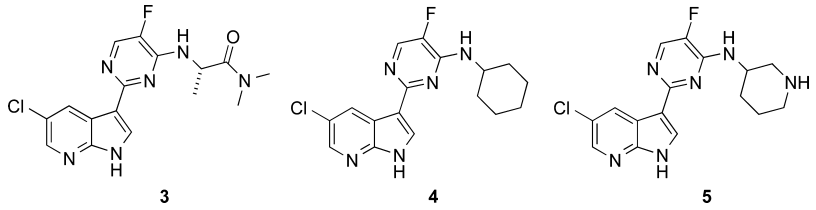

Figure 2. Azaindole screening hits.

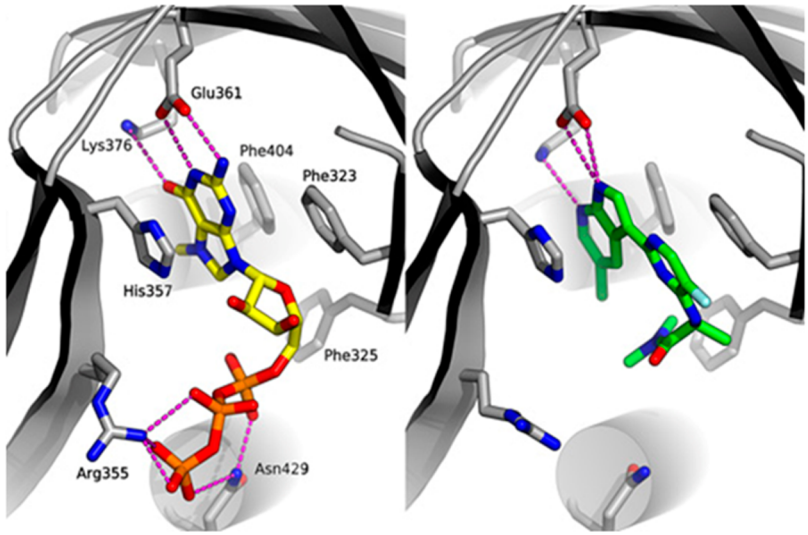

Figure 3. X-ray structure of cap-binding domain (contact residues) of PB2 containing 7-methyl GTP (left) or **3** (right). Accession codes are the following: 4NCE for 7-methyl GTP and 4NCM for **3**.

has generated significant concern,[6] especially with the report that the H5N1 influenza virus has shown resistance to oseltamivir,[7] reinforcing the critical need for new anti-influenza therapeutics with novel mechanisms of action.

RESULTS AND DISCUSSION

The goal of our program was to develop a novel dual route (iv and oral) inhibitor for the treatment of influenza that specifically addresses the shortcomings of the current standard of care. To this end, we started our program by utilizing a phenotypic cell protection (CPE) assay to identify screening hits that could overcome the viral challenge limitation of the neuraminidase inhibitors.[8] An initial screen of 1000 compounds (selected based on their cellular activity in various assays and the lack of cytotoxicity) identified numerous compounds with measurable antiviral activity. In particular, a series of 3-pyrimidineazaindoles with significant cell protective activity at 10 μM concentration emerged from the screen. Subsequent rounds of screening identified multiple subclasses that were selected for exploratory chemistry. Three subclasses of interest can be exemplified by the hits shown in Figure 2.

Subsequently, the molecular target of this compound class was determined to be the PB2 subunit of the influenza viral polymerase.[9] The viral polymerase contains three subunits, PB1, PB2, and PA, that are responsible for replication and transcription of the eight separate segments of the viral RNA genome in the nuclei of infected cells.[9,10] The heterotrimeric viral polymerase synthesizes viral mRNAs via a unique "cap-snatching" mechanism where the virus utilizes host pre-mRNA as a primer for transcription.[11] The PB2 subunit contains a cap binding domain for 7-methyl GTP (m^7GTP) on the 5′-end of the host pre-mRNA. Once bound to PB2, the PA endonuclease subunit cleaves the host RNA strand, leaving a 10−13 nucleotide primer. The PB1 subunit contains the conserved polymerase domain and utilizes the primer for RNA elongation. Soon after identification of PB2 as the target for these azaindole screening hits, the X-ray crystal structures of m^7GTP and VRT-0761704 (**3**) bound to the PB2 cap-binding domain were determined (Figure 3). Though belonging to a different space group (see Supporting Information), the structure of the PB2 cap binding fragment was consistent with that previously described for complexes with m^7GTP.[9] This new structure revealed that **3** occupies the m^7GTP binding site and produces similar interactions with the protein as the m^7GTP guanine base (Figure 3). Both m^7GTP and **3** form hydrogen bonds to the side chains of Glu361 and Lys376. The azaindole of **3** is sandwiched between the aromatic side chains of His357 and Phe404, while the pyrimidine π-stacks against Phe323. The dimethylalanyl portion of **3** is located near the region occupied by the m^7GTP ribose and α-phosphate. We observed no direct polar interactions of **3** with the positively charged residues (Lys-339, Arg-355, and His-357) located in the m^7GTP phosphate binding region, which became an area for exploration discussed later in this paper.

In the early stages of our project we established that optimal and consistent cellular potency was achieved with chloro substitution at the 5-position of the azaindole ring system (Cl > F > H; see discussion later in text). On the basis of our analysis of the crystal structure and additional azaindole screening hits, we focused our optimization efforts on the amino substituent at the 4-position of the pyrimidine ring system. Initial analogues, such as cyclohexylamine, **4** (Table 1), maintained potency relative to **3**. Additionally, we observed a preference for six-

dx.doi.org/10.1021/jm5007275 | J. Med. Chem. 2014, 57, 6668−6678

Table 1. Optimization of in Vitro Potency of Cycloalkyl and Piperidine Based 5-Chloroazaindole Inhibitors

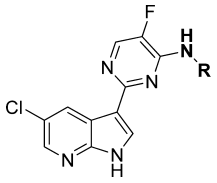

Compd	Amine (NH-R)	CPE EC_{50}[a] (μM)	bDNA EC_{90}[b] (μM)	PB2 Kd[c] (μM)
3	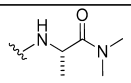	0.51	1.13	0.10
4	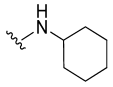	1.64	2.37	0.30
5	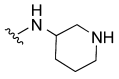	1.87	--	--
6	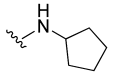	>20	> 10	0.70
7	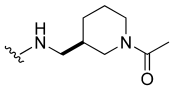	0.40	0.54	0.30
8	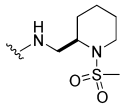	0.66	0.54	0.10
9	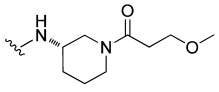	0.013	0.32	0.10
10	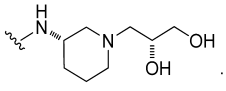	0.27	0.36	0.40
11	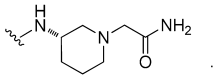	0.081	0.02	0.08

[a]MDCK cells were incubated with test compounds and influenza A virus (A/PR/8/34 strain) for 72 h, and the concentration of test compound resulting in 50% cell protection was reported as the EC_{50}. [b]The concentration of test compound resulting in viral RNA levels equal to that of 10% of the control wells was reported as EC_{90}. [c]Affinity for cap-binding domain of the PB2 subunit as measured in a fluorescence polarization competition binding assay.

membered cycloalkyl over smaller rings (compound **6**). We then identified additional potent compounds in the bDNA assay[1] having substituted cycloheteroalkylamines on the pyrimidine ring (Table 1), highlighted by the aminopiperidine and aminomethylpiperidine subseries (compounds **7**–**11**). Our hypothesis for the observed improvement in potency was due to the hydrophobic portion of the piperidine rings more efficiently occupying the aforementioned hydrophobic pocket coupled with a potential interaction of the acyl/sulfonamide groups with Asn-429. We also observed a stereochemical preference: (*S*)-stereochemistry for the aminopiperidines and (*R*)-stereochemistry for the aminomethylpiperidines. These analogues, typically capped with an amide, urea, or sulfonamide, consistently showed high clearance in rat PK studies (compounds **8** and **9**, Table 6). In an effort to improve potency (through potential interactions with the His-357, Lys-339, and Arg-355 residues in the GTP phosphate binding region), increase solubility, and reduce clearance thought to be associated with the amido-capped piperidines, we designed a set of *N*-alkylpiperidines, highlighted by piperidines **10** and **11**. The *N*-alkylacetamide analogue **11** showed the strongest cellular (bDNA) and enzyme binding potency of any compound in this series; however, **11** also showed high clearance in rats (182 mL min^{-1} kg^{-1}). The diol **10** was the first compound in this series to display reasonable potency in the bDNA assay and show an acceptable improvement in clearance and half-life (rat) as well as reasonable oral exposure in mouse (Table 6). Our initial pharmacology studies with **10** in a mouse pretreatment influenza model showed efficacy at high doses (data not shown). These observations were exciting but showed that further optimization of potency and pharmacokinetics was still required.

Synthesis of the azaindolepiperidine diol **10** was accomplished in eight steps from the commercially available bromide **12** (Scheme 1). Protection of the azaindole NH functionality as a tosylate followed by reaction with bis(pinacolato)diboron afforded the boronate ester **13**. Suzuki coupling with 2-chloro-5-fluoro-4-methylthiopyrimidine, **14**, provided the methyl sulfide **15**. Oxidation of the sulfide to the sulfoxide **16** allows for facile displacement with Boc-protected (*S*)-3-aminopiperidine. Removal of the Boc-protecting group followed by alkylation of the free piperidine NH with (*S*)-glycidol affords the desired piperidine diol **14** after base-catalyzed removal of the tosyl protecting group.

During the course of our lead optimization efforts, we evolved from the piperidine-based analogues to 1,2- and 1,3-diaminocyclohexyl analogues (Table 2). Our goal was to maintain the putative interactions made by the piperidine acyl/sulfonamide groups while improving metabolic stability by moving the nitrogen out of the ring. These analogues showed a more consistent boost in cellular (bDNA) potency, relative to the aminopiperidine analogues, as well as improvement in metabolic stability (data not shown). The preference for the (*S*)-stereochemistry adjacent to the pyrimidine ring was maintained in this subseries (compounds **18** and **19**) as reflected in both the cell protection and PB2 fluorescent binding assays.[14] While the PB2 binding data were useful in prioritizing each of the subseries of azaindoles that were explored, the PB2 data did not always reflect the potency trends observed in the cellular bDNA assays,[14] which became the primary assay for driving the SAR on this project. In general, the 1,3-diaminocyclohexyl analogues displayed a more robust SAR tolerance than the 1,2-diaminocyclohexyl analogues, exemplified by the >50-fold boost in potency in the bDNA assay (**20** vs **21**). Therefore, we focused our attention on derivatization of the 3-amino functionality. The preferred stereochemical relationship of the 1,3-diamino group was established as cis (data not shown). Capping of the 3-amino group with simple amides resulted in a significant boost in bDNA potency (compounds **21**–**23**), while more solubilizing amides were less potent (compounds **24** and **25**). The most potent compounds in this series came in the form of tertiary

dx.doi.org/10.1021/jm5007275 | J. Med. Chem. 2014, 57, 6668–6678

Scheme 1. Synthetic Scheme for 5-Chloroazaindolepyrimidinyl Piperidine Analogue 10[a]

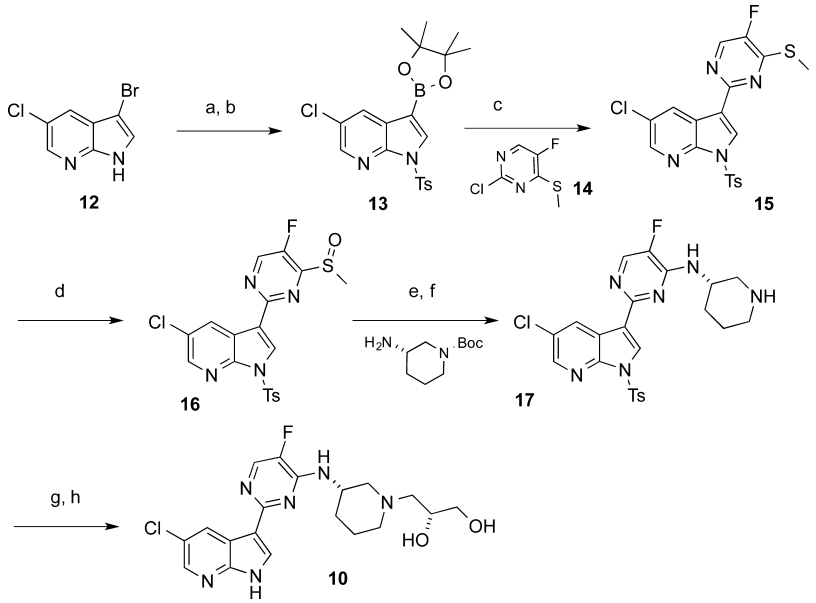

[a]Reagents and conditions: (a) NaH, TsCl, DMF, 85%; (b) bis(pinacolato)diboron, KOAc, $PdCl_2$(dppf), dioxane, water, reflux, 50%; (c) **14**, $Pd(PPh_3)_4$, Na_2CO_3, DME, water, 94%; (d) mCPBA, CH_2Cl_2, 96%; (e) (*S*)-3-amino-1-Boc piperidine, $^iPr_2NEt$, DMF, 90 °C, 60%; (f) TFA, CH_2Cl_2, 95%; (g) (*S*)-(−)-glycidol, EtOH, microwave, 140 °C, 58%; (h) NaOMe, MeOH, 45%.

substituted urea analogues, such as compounds **26**−**28**, compared to the secondary urea **29**. Additionally, *N*-methylimidazoleamides **30** and **31** showed equivalent potency.

It is worth noting that these more potent ureas (**27** and **28**) and amides (**30** and **31**) only showed a small difference in potency between the 5-chloro and 5-fluoroazaindole substitutions. Table 3 shows a summary of SAR at the 5-position of the azaindoles. Generally, small halo- or haloalkyl substituents at the 5-position (compounds **27**, **28**, and **33**) displayed the best potency, while the methyl ketone, **34**, showed the least activity in this set. A simple 5-methyl substitution (compound **35**) retains potency better than larger alkyl groups, hydrogen or electron donating groups (compounds **36**, **37** and **38**) with the most significant drop-off in potency among these small substituents occurring with 5-substituted *N*,*N*-dimethylamine (compound **39**). A direct comparison of rat iv clearance values of the four most potent analogues in Table 3 (compounds **27**, **28**, **33**, and **35**) showed a clear preference for the 5-fluoro substitution. The improved clearance values, along with the observation that the 5-fluoroazaindoles generally showed improvements in kinase selectivity, aqueous solubility, and oral exposure in rodents, helped better guide the program, even though earlier, less potent analogues showed a greater difference in potency between 5-chloro and 5-fluoro.

The pharmacokinetic profile of **28** showed encouraging oral exposure in both rat and mouse (Table 6). This compound was advanced into a mouse influenza model (Figure 4) showing 75% survival in a +48 h delay to treatment model (30 mpk b.i.d. × 10 days). The corresponding C_{min} following the 30 mpk b.i.d. regimen was 370 μM, approximately 30-fold over the in vitro EC_{90}. The efficacy observed with **28** was an improvement over the current SOC, oseltamivir. When dosing oseltamivir at the clinically relevant human equivalent dose (10 mpk b.i.d.) in the same +48 h delay-to-treatment model, oseltamivir provided no survival benefit (single dose PK of oseltamivir carboxylate (10 mpk in healthy Balb/C mouse) AUC = 3.8 μg·h/mL, C_{max} = 2520 ng/mL).

A concerted effort was initiated to explore chemical diversity on the aminocyclohexyl ring system. A breakthrough was achieved during our exploration of the 1,2-diaminocyclohexane analogues. We reversed the 2-acetamido functionality of **20** to give the β-aminocarboxamide **40** (Table 4), which showed similar potency in the bDNA assay. While moderate improvements in potency were observed by exploring amide substitutions (data not shown), the turning point in this series came when we designed the carboxylic acid analogue **41**. The structural information shown in Figure 2 had suggested that if we could incorporate a negatively charged moiety into the phosphate-binding region of GTP, this might result in strong interactions with the corresponding basic residues (His-357, Lys-339, and Arg-355). Compound **41** proved to be the most potent ligand we had seen in the PB2 fluorescent polarization binding assay, exceeding the sensitivity limits of the assay (K_d < 0.002 nM). The compound also exhibited a significant increase in cellular potency (16-fold in bDNA assay relative to **40**). While this compound also showed exquisite selectivity vs kinases and receptors, it showed limited oral exposure in rats (Table 6) as well as an unfavorable efflux ratio (Caco-2 efflux ratio of 13). In an attempt to increase lipophilicity around the carboxylic acid functionality, in order to increase cell penetration and consequently improve cell potency as well as increase oral exposure, we designed geminal substituted carboxylic acid analogues **42**−**44**, all of which either maintained or slightly increased cellular potency. The simple geminal-methyl analogue **42** showed reduced efflux (Caco-2 ratio of 2), presumably due to increasing lipophilicity and bulk around the acid moiety[15] and improved oral exposure in rats (Table 6). A significant breakthrough in this optimization path was the design of the bridged cyclohexyl analogues. We further optimized the van der Waals interactions in the hydrophobic portion in the PB2 binding site and achieved better balance

dx.doi.org/10.1021/jm5007275 | J. Med. Chem. 2014, 57, 6668−6678

Table 2. Optimization of in Vitro Potency of Diamino Cyclohexyl-Based Inhibitors

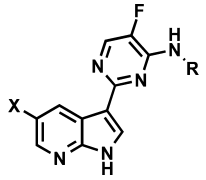

Compd	Amine (NH-R)	X	CPE EC_{50} (μM)[a]	bDNA EC_{90} (μM)[b]	PB2 Kd (μM)[c]
18		Cl	0.62	2.48	0.09
19		Cl	>20	--	4.90
20	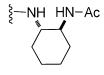	Cl	0.044	1.46	0.10
21	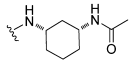	Cl	0.036	0.025	0.07
22	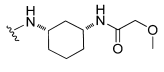	Cl	0.044	0.02	0.07
23		F	0.045	0.09	0.20
24	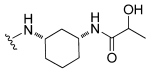	Cl	0.086	0.24	0.40
25	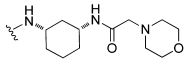	Cl	0.100	0.38	0.20
26	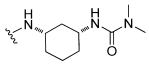	F	0.002	0.006	0.40
27	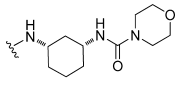	Cl	0.002	0.005	0.50
28		F	0.004	0.012	0.40
29	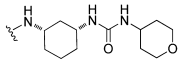	F	0.06	0.16	0.40
30	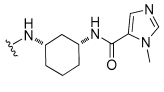	Cl	0.002	0.003	0.02
31		F	0.002	0.005	0.09

[a]MDCK cells were incubated with test compounds and influenza A virus (A/PR/8/34 strain) for 72 h, and the concentration of test compound resulting in 50% cell protection was reported as the EC_{50}. [b]The concentration of test compound resulting in viral RNA levels equal to that of 10% of the control wells was reported as EC_{90}. [c]Affinity for cap-binding domain of the PB2 subunit as measured in a fluorescence polarization competition binding assay.

between the lipophilicity of the molecule vs the acidic functionality. The single carbon bridged analogues **45** and **46** showed a further increase in cellular potency, with a slight preference for the *endo*-product **46**. The [2,2,2]bicyclooctane analogues **47** and **2** afforded the most potent compounds in the program with bDNA EC_{90} values of <5 nM as well as the added advantage of lack of *endo* and *exo* stereoisomers with the symmetric [2,2,2] system.

Table 3. SAR of 5-Substituted Azaindole Inhibitors

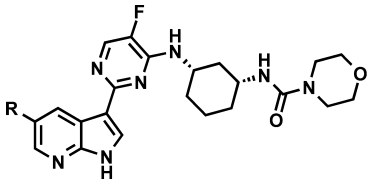

compd	R	CPE EC_{50} [a] (μM)	bDNA EC_{90} [b] (μM)	rat iv Cl (mL min^{-1} kg^{-1})
27	Cl	0.002	0.005	59
28	F	0.004	0.012	22
33	CF_3	0.003	0.003	81
34	C(O)Me	>10	>3	
35	CH_3	0.010	0.013	78
36	CH_2CH_3	0.025	0.260	
37	OMe	0.095	0.170	
38	H	0.098	0.200	
39	NMe_2	1.260	>3	

[a]MDCK cells were incubated with test compounds and influenza A virus (A/PR/8/34 strain) for 72 h, and the concentration of test compound resulting in 50% cell protection was reported as the EC_{50}. [b]The concentration of test compound resulting in viral RNA levels equal to that of 10% of the control wells was reported as EC_{90}.

Compound **2**, designated VX-787,[12] also demonstrates potent, antiviral activity in vitro (CPE assay) against a broad range of influenza type A strains,[13] including neuraminidase inhibitor and amantadine resistant isolates and current pandemic H1N1 and H5N1 strains (Table 5). The activity appears to be specific for influenza A virus, as neglible activity against influenza B virus was observed (data not shown).

The X-ray crystal structure of **2** bound to PB2 confirmed that the azaindole ring system makes the expected interactions with the protein residues Lys-376 and Glu-361 as well as stacking of the three aromatic rings of **2** between the side chains of His-357, Phe-323, and Phe-404 (Figure 5). The carboxylic group of the ligand makes two water-mediated interactions with the ε nitrogen of His 357 and with Gln-406 as well as the main chain carbonyl of Arg-355. Additional interactions with Lys-339 and Arg-355 in the adjacent region were expected, consistent with the substantial increase in binding affinity imparted by the carboxylic group. However, no direct interactions between the ligand and these basic residues were observed in the structure. We hypothesized that the low pH and high salt concentration of the crystallographic buffer (3 M sodium formate, pH 4.5) may have masked these interactions. While SPR experiments showed that the binding affinity of the related acid **41** was not significantly affected by these factors, no confirmatory crystal structure at low salt and neutral pH could be obtained.

Scheme 2 depicts the synthesis of **2** using a more convergent process of coupling the azaindole boronate species toward the end of the sequence. The synthesis of the enantiomerically pure β-amino ester pyrimidine fragment **55** was accomplished in five steps, followed by a chromatographic resolution (Scheme 2). The sequence begins with a Diels–Alder cycloaddition between maleic anhydride and 1,3-cyclohexadiene. The resulting *endo* cycloaddition product **50** was stirred for 4 days under basic conditions to open the anhydride and epimerize the resulting ester to afford the desired trans ester carboxylic acid product **51** as a racemic mixture. Curtius rearrangement with subsequent trapping with benzyl alcohol provided the protected cyclic amino acid **52**. Hydrogenation of **52** yielded the bridged

dx.doi.org/10.1021/jm5007275 | J. Med. Chem. 2014, 57, 6668–6678

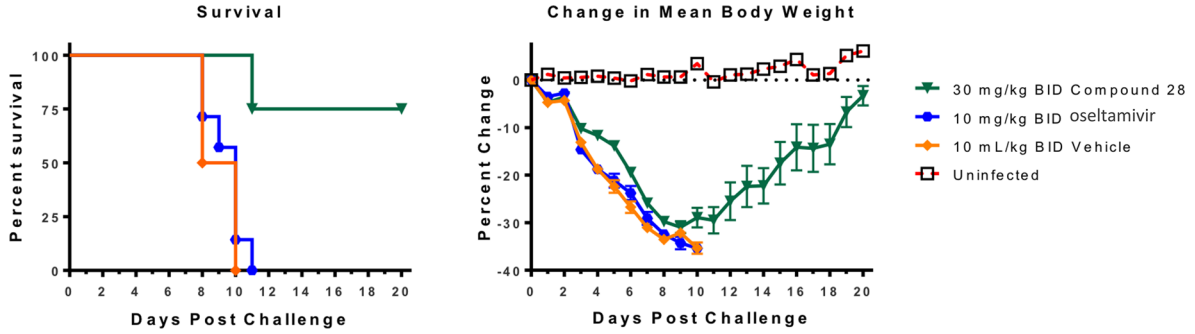

Figure 4. In vivo activity of **28** and oseltamivir in mouse influenza A model when administered 48 h after infection: survival and body weight curves of male BALB/C mice (8 mice/group) inoculated with mouse-adapted influenza viruses A/PR/8/34 (5e3 $TCID_{50}$/mouse) by intranasal instillation.

Table 4. Optimization of in Vitro Potency of Cyclohexyl Carboxylate Based Inhibitors

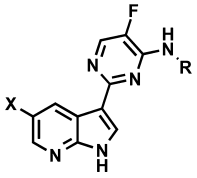

Compd	Amine (NH-R)	X	CPE EC_{50} (μM)[a]	bDNA EC_{90} (μM)[b]	PB2 Kd (μM)[c]
40	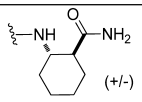	Cl	--	3.13	0.03
41	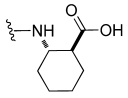	Cl	0.134	0.187	<0.002
42	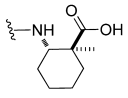	Cl	0.011	0.059	<0.002
43		F	0.018	0.140	<0.002
44	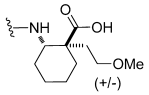	Cl	0.018	0.09	0.009
45	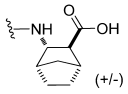	Cl	0.008	0.021	<0.002
46	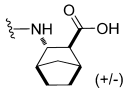	Cl	<0.002	0.006	<0.002
47	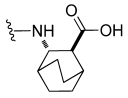	Cl	0.001	0.001	<0.005
2		F	0.002	0.004	<0.003

[a]MDCK cells were incubated with test compounds and influenza A virus (A/PR/8/34 strain) for 72 h, and the concentration of test compound resulting in 50% cell protection was reported as the EC_{50}. [b]The concentration of test compound resulting in viral RNA levels equal to that of 10% of the control wells was reported as EC_{90}. [c]Affinity for cap-binding domain of the PB2 subunit as measured in a fluorescence polarization competition binding assay.

Table 5. Compound 2 Maintains Antiviral Potency vs Adamantine and NAI Resistant Viruses

	mean CPE EC_{50} (μM)[a]		
virus	**2**	amantadine	oseltamivir carboxylate
A/Georgia/20/2006	0.0026	>10	>10[d]
A/Texas/48/2009[b]	0.0028	>10	>10[d]
A/Puerto Rico/8/34	0.000 32	>10[d]	>10
A/California/07/2009[b]	0.0018	>10[d]	>10
A/Mexico/4108/2009[b]	0.0027	>10[d]	>10
A/New York/18/2009[b]	0.000 59	>10[d]	0.16
A/Viet Nam/1203/2004[c]	<0.00015[e]	ND[f]	ND[f]

[a]Mean MDCK cell 3-day CPE assay EC_{50}, $N = 3$ or greater. [b]Influenza A (H1N1) 2009 pandemic strain. [c]Highly pathogenic avian influenza (H5N1) strain. [d]Resistant, determined via externally validated phenotypic or genetic analysis. [e]Performed at Southern Research Institute. [f]ND: not determined.

cyclohexylamino ester **53**. After coupling with 2,4-dichloro-5-fluoropyrimidine, chromatography on a chiral support was utilized to separate the enantiomers. With the (*S*,*S*) bridged cyclohexylamino-chloropyrimidine **55** in hand, a Suzuki cross-coupling with the 5-fluoroazaindole boronate ester fragment, **56**,[12] gives the fully assembled scaffold **57**, which upon removal of the tosylate protecting group and hydrolysis of the ester provided **2** in eight overall steps.

As mentioned earlier, one of the advantages of the carboxylic acid analogues is a superior selectivity profile. PB2 inhibitor **2** was tested against a panel of kinases (65) and only showed measurable inhibition (K_i = 1.6 μM) against a single kinase, GSK3β (see Supporting Information). Additionally, **2** was evaluated for interaction with a variety of receptors, ion channels, and other targets (68 total) and was shown to bind competitively to only two of these targets at 10 μM: adenosine A1 (96% inhibition) and A2a (62% inhibition). No inhibition was observed with **2** against either hERG (manual patch, >30 μM) or a panel of CYPs (>30 μM). The pharmacokinetic profile of **2** showed good oral exposure in both rat and mouse.

Compound **2** was advanced into a mouse influenza model where it showed 100% survival in the +48 h delay to treatment model at 10, 3, or 1 mpk (b.i.d. × 10 days), whereas the SOC oseltamivir provided no survival benefit in this model at 10 mpk (Figure 6). Compound **2** also showed a marked improvement in observed body weight loss (BWL) with a loss of 7.1% at 10 mpk, 10.9% at 3 mpk, and 22.5% at 1 mpk on study day compared to **28** administered at an even higher dose (30 mpk) (~30% BWL). Again, oseltamivir was run in the same +48 h delayed treatment model and showed 0% survival and greater

dx.doi.org/10.1021/jm5007275 | J. Med. Chem. 2014, 57, 6668−6678

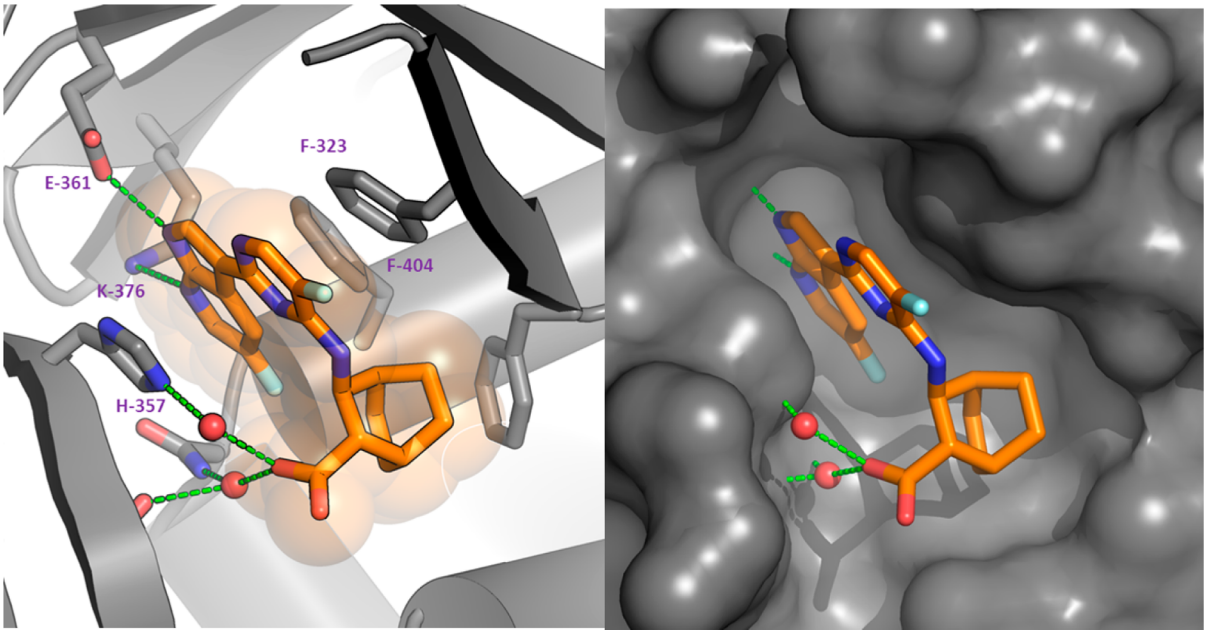

Figure 5. X-ray structure of **2** bound to PB2. Accession code is 4P1U.

Scheme 2. Synthetic Scheme for 2[a]

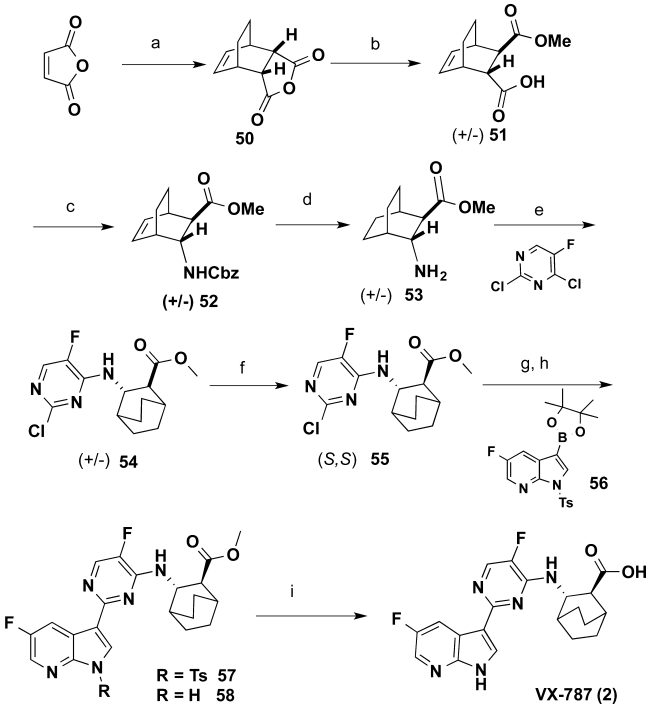

[a]Reagents and conditions: (a) $CHCl_3$, 78%; (b) NaOMe, MeOH, 4 days, 85%; (c) DPPA, Et_3N, BnOH, 77%; (d) H_2, Pd/C, THF/MeOH, 99%; (e) 2,4-dichloro-5-fluoropyrimidine, $^iPr_2NEt$, THF, 77%; (f) SFC chiral separation; (g) **56**, $Pd_2(dba)_3$, K_3PO_4, 2-MeTHF, water, 120 °C, 95%; (h) HCl, dioxane, MeCN, 95%; (i) NaOH, THF, MeOH, 95%.

than 30% BWL loss at 10 mpk b.i.d. The efficacy observed with **2** not only represents a significant improvement over earlier compounds, such as **28**, but a dramatic improvement over the current SOC, oseltamivir, at this higher viral challenge dose. Compound **2** exhibited greater efficacy than **28** in its protection against the drastic body weight loss in the infected animals. The

Table 6. Mouse and Rat PK Parameters for Selected PB2 Influenza Inhibitors

	rat (3 mg/kg)		mouse (30 mg/kg)	
compd	iv Cl,[d] $T_{1/2}$(h)	po AUC,[b] C_{max},[c] % F	AUC[b]	C_{max} [c]
8	152, 0.4			
9	88, 0.7			
10	56, 2.3		6.5	1.2
28	22, 1.7	1.1, 0.2, 46	180	18.2
31	22, 2	3.7, 0.6, 100	19	13
41[a]	16, 1	0.2, 0.03, 7		
42[a]	24, 3.2	2.2, 0.2, 82	2.4	1.3
47	32, 3.9	0.3, 0.03, 24	10	3.7
2	26, 3.5	0.5, 0.08, 26	22	18

[a]Rat PK data obtained from racemic mixture. [b]AUC measured (μg·h/mL). [c]Normalized to actual dose (μg/mL). [d]Cl measured (mL min^{-1} kg^{-1}).

improvement is more apparent when compared on an equivalent exposure basis (Table 6). Additionally, **2** shows efficacy beyond +48 h in this treatment model, results that will be described in an upcoming publication.[13]

■ CONCLUSIONS

Starting from a phenotypic screening effort using a cell protection assay, a class of azaindole-based compounds was identified that was found to be inhibitors of the PB2 subunit of the influenza A viral polymerase complex. Structure guided optimization led to the design of a set of cyclohexylcarboxylic acid analogues, highlighted by **2**. Compound **2** was found to be an orally bioavailable, extremely potent, and efficacious inhibitor with a clean selectivity profile. Further testing showed **2** was extremely potent versus all influenza A strains tested, including pandemic H1N1 and avian H5N1 flu strains. The overall profile of **2**, coupled with an early acting mechanism in the influenza viral life cycle, translated into unprecedented efficacy in a +48 h treatment mouse influenza model. This data clearly indicate that **2** is a first-in-class influenza inhibitor that is superior to the current standard-of-care agent oseltamivir with

dx.doi.org/10.1021/jm5007275 | J. Med. Chem. 2014, 57, 6668−6678

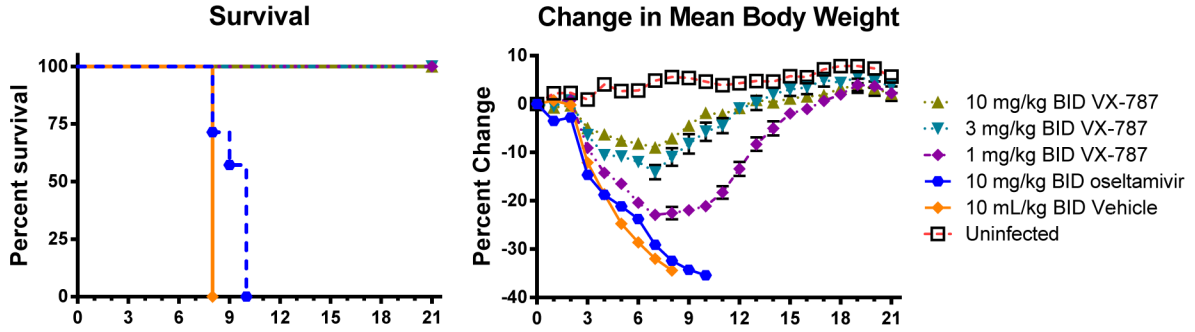

Figure 6. In vivo activity of **2** and oseltamivir in mouse influenza A model when administered 48 h after infection: survival and body weight curves of male BALB/C mice (8 mice/study) inoculated with mouse-adapted influenza viruses A/PR/8/34 (5e3 $TCID_{50}$/mouse) by intranasal instillation.

respect to overall potency, efficacy, and extended treatment window. It is believed that **2** possesses great therapeutic potential and is being evaluated in clinical trials.

EXPERIMENTAL SECTION

All commercially available reagents and anhydrous solvents were used without further purification. Purity assessment for final compounds was based on analytical HPLC: 4.6 mm × 50 mm Waters YMC Pro-C18 column, 5 μm, 120A. Mobile phases are as follows: A, H_2O with 0.2% formic acid; B, acetonitrile with 0.2% formic acid; gradient, 10−90% B in 3 min with 5 min run time. The flow rate is 1.5 mL/min. Unless specified otherwise, all compounds were ≥95% pure. Mass samples were analyzed on a Micro Mass ZQ, ZMD, Quattro LC, or Quatro II mass spectrometer operated in a single MS mode with electrospray ionization. Samples were introduced into the mass spectrometer using flow injection (FIA) or chromatography. The mobile phase for all mass analysis consisted of acetonitrile−water mixtures with either 0.2% formic acid or ammonium formate. ^{1}H NMR spectra were recorded using either a Bruker Avance 400 (400 MHz) or a Bruker Avance II-300 (300 MHz) instrument. The column chromatography was performed using Teledyne ISCO RediSep normal phase (35−70 μm) or RediSep Gold normal phase (25−40 μm) silica flash columns using a Teledyne ISCO Combiflash Companion or Combiflash Rf purification system. Preparative reversed phase chromatography was carried out using a Gilson 215 liquid handler coupled to a UV−vis 156 Gilson detector, an Agilent Zorbax SB-C18 column, 21.2 mm × 100 mm, with a linear gradient from 10% to 90% CH_3CN in H_2O over 10 min (0.1% trifluoroacetic acid). The flow rate was 20 mL/min.

5-Chloro-3-(4,4,5,5-tetramethyl-1,3,2-dioxaborolan-2-yl)-1-tosyl-1*H*-pyrrolo[2,3-*b*]pyridine (13). Sodium hydride (2.2 g, 54.0 mmol) was added portionwise to a cold (0 °C) solution of 3-bromo-5-chloro-l*H*-pyrrolo[2,3-*b*]pyridine, **12** (10.5 g, 45.0 mmol), in dimethylformamide (70 mL) under a nitrogen atmosphere. After the mixture was stirred at room temperature for 30 min, tosyl chloride (8.7 g, 46.0 mmol) was added to the mixture and the mixture was stirred at room temperature for 18 h. The reaction mixture was quenched with water (150 mL) and the resulting brown solid was filtered and dried under vacuum to afford 3-bromo-5-chloro-1-tosyl-1*H*-pyrrolo[2,3-*b*]pyridine (14.8g, 85%): ^{1}H NMR ($CDCl_3$) 8.4 (s, 1H), 8.1−82 (d, 2H), 7.8−7.9 (d, 2H), 7.3−7.4 (d, 2H), 2.4 (3H, s); MS(ES+) 387.

A 500 mL round-bottom flask under a nitrogen atmosphere was charged with 3-bromo-5-chloro-1-tosyl-1*H*-pyrrolo[2,3-*b*]pyridine (6.9 g, 18.0 mmol), bispinacolatodiboron (6.9 g, 27.0 mmol), $PdCl_2(dppf)_2$ (1.5 g, 2.0 mmol), potassium acetate (5.3 g, 54.0 mmol), and dimethoxyethane (100 mL). The reaction mixture was stirred at 90 °C for 18 h. The reaction mixture was diluted with ethyl acetate (200 mL) and washed with brine. The organic phase was dried over magnesium sulfate, filtered, and concentrated in vacuo. The resulting residue was purified by silica gel chromatography, using as eluent pentane/EtOAc 0−20% and then triturated with pentane to afford **13** (4g, 50%): ^{1}H NMR ($CDCl_3$) 8.30 (s, 1H), 8.10 (s, 2H), 8.00−8.05 (d, 2H), 7.20 (d, 2H), 2.40 (s, 3H), 1.40 (s, 9H); MS(ES+) 433.

5-Chloro-3-(4,4,5,5-tetramethyl-1,3,2-dioxaborolan-2-yl)-1-tosyl-1*H*-pyrrolo[2,3-*b*]pyridine (56). Using the same procedure described above and substituting 3-bromo-5-fluoro- l*H*-pyrrolo[2,3-*b*]pyridine instead of 3-bromo-5-chloro-l*H*-pyrrolo[2,3-*b*]pyridine afford the desired product, **56**: ^{1}H NMR ($CDCl_3$) 8.45 (s, 1H), 8.15 (s, 2H), 8.10 (d, 2H), 7.85 (d, 1H), 7.45 (d, 2H), 2.32 (s, 3H), 1.33 (s, 9H); MS(ES+) 417.

5-Chloro-3-(5-fluoro-4-(methylthio)pyrimidin-2-yl)-1-tosyl-1*H*-pyrrolo[2,3-*b*]pyridine (15). 2-Chloro-5-fluoro-4-methylsulfanylpyrimidine, **14** (0.64 g, 3.60 mmol), 5-chloro-3-(4,4,5,5-tetramethyl-1,3,2-dioxaborolan-2-yl)-1-tosyl-1*H*-pyrrolo[2,3-*b*]pyridine, **13** (1.30 g, 3.0 mmol), and aqueous Na_2CO_3 (4.5 mL of 2 M solution, 9.0 mmol) were dissolved in DME (14 mL). The mixture was purged with nitrogen for 15 min, treated with $Pd(PPh_3)_4$ (0.17 g, 0.15 mmol), and heated in a pressure tube at 125 °C for 15 min. After the mixture was cooled to room temperature, the resulting precipitate was filtered and washed with methanol to afford **15** (1.27 g, 94%): ^{1}H NMR (400 MHz, $CDCl_3$) δ 8.80 (d, J = 2.4, 1H), 8.60 (s, 1H), 8.40 (d, J = 2.4, 1H), 8.25 (d, J = 1.7, 1H), 8.19−8.03 (m, 2H), 7.30 (d, J = 8.1, 2H), 2.74 (s, 3H), 2.39 (s, 3H); MS (ES+) 449.3.

5-Chloro-3-(5-fluoro-4-(methylsulfinyl)pyrimidin-2-yl)-1-tosyl-1*H*-pyrrolo[2,3-*b*]pyridine (16). To a cold (0 °C) solution of 5-chloro-3-(5-fluoro-4-(methylthio)pyrimidin-2-yl)-1-tosyl-1*H*-pyrrolo[2,3-*b*]pyridine, **15** (56.0 g, 124.7 mmol), in dichloromethane (2.5 L) was added portionwise 3-chlorobenzenecarboperoxoic acid (31.0 g, 131.1 mmol). The internal temperature was maintained below 5 °C. The resulting reaction mixture was slowly allowed to warm to ambient temperatue over 4 h. The reaction mixture was quenched with 10% aqueous $NaHSO_3$ solution (150 mL) and stirred for 30 min. The organic layer was separated, washed with aqueous saturated $NaHCO_3$ solution (2 × 600 mL), brine (600 mL), dried over Na_2SO_4, filtered, and concentrated under reduced pressure. The resulting crude residue was triturated with MTBE (2 × 150 mL) to afford the desired product **16** (55.4 g. 96% yield) as a white solid: ^{1}H NMR (DMSO-d_6) δ 9.12 (s, 1H), 8.89 (d, J = 3 Hz, 1H), 8.67 (s, 1H), 8.53 (d, J = 3 Hz, 1H), 8.12 (d, J = 9 Hz, 2H), 7.46 (d, J = 9 Hz, 2H), 3.06 (s, 3H), 2.36 (s, 3H).

(*S*)-2-(5-Chloro-1-tosyl-1*H*-pyrrolo[2,3-*b*]pyridin-3-yl)-5-fluoro-*N*-(piperidin-3-yl)pyrimidin-4-amine (17). To a solution of 5-chloro-3-(5-fluoro-4-(methylsulfinyl)pyrimidin-2-yl)-1-tosyl-1*H*-pyrrolo[2,3-*b*]pyridine, **16** (4.0 g, 8.6 mmol), and *tert*-butyl (3*S*)-3-aminopiperidine-1-carboxylate (2.1 g, 10.3 mmol) in DMF (50 mL) was added diisopropylethylamine (3.0 mL, 17.2 mmol). The reaction mixture was heated at 80 °C for 18 h. The mixture was cooled to room temperature and diluted into aqueous saturated NH_4Cl solution and extracted twice with EtOAc. The combined organic phases were washed with brine (3 times), dried ($MgSO_4$), filtered, and concentrated under vacuum. The resulting residue was purified via silica gel chromatography (0%−80% EtOAc/hexanes) to afford the intermediate piperidine: ESI-MS m/z calcd 601.5, found 601.43 (M + 1).

To a solution of *tert*-butyl (3*S*)-3-[[2-[5-chloro-1-(*p*-tolylsulfonyl)-pyrrolo[5,4-*b*]pyridin-3-yl]-5-fluoropyrimidin-4-yl]amino]piperidine-1-carboxylate (2.1 g, 3.5 mmol) in CH_2Cl_2 (30 mL) was added

dx.doi.org/10.1021/jm5007275 | J. Med. Chem. 2014, 57, 6668−6678

trifluoroacetic acid (20 mL). After the reaction mixture was stirred at room temperature for 75 min, the mixture was concentrated under vacuum. The crude residue was diluted with EtOAc and neutralized with 1 N sodium hydroxide solution. The aqueous phase was separated and extracted again with EtOAc. The combined organic phases were dried ($MgSO_4$), filtered, and concentrated under vacuum to afford the desired product, **17**, as a light yellow solid: ^{1}H NMR (300 MHz, DMSO-d_6) δ 8.76 (d, J = 2.5, Hz, 1H), 8.50 (d, J = 2.5 Hz, 1H), 8.44 (s, 1H), 8.27 (d, J = 4.0 Hz, 1H), 8.06 (d, J = 8.5 Hz, 2H), 7.66 (d, J = 6.9 Hz, 1H), 7.45 (d, J = 8.2 Hz, 2H), 4.17 (m, 1H), 3.17 (dd, J = 3.1, 11.8 Hz, 1H), 2.99−2.94 (m, 1H), 2.67−2.60 (m, 1H), 2.38−2.34 (m, 1H), 2.06−2.02 (m, 1H), 1.77−1.73 (m, 1H), and 1.63−1.50 (m, 2H) ppm; LCMS t_R = 2.1 min, (M + 1) 501.5, (M − 1) 499.5.

(*R*)-3-((*S*)-3-((2-(5-Chloro-1-tosyl-1*H*-pyrrolo[2,3-*b*]pyridin-3-yl)-5-fluoropyrimidin-4-yl)amino)piperidin-1-yl)propane-1,2-diol (17b). To a solution of (*S*)-2-(5-chloro-1-tosyl-1*H*-pyrrolo[2,3-*b*]pyridin-3-yl)-5-fluoro-*N*-(piperidin-3-yl)pyrimidin-4-amine, **17** (2.22 g, 4.43 mmol), in ethanol was added (*S*)-glycidol (0.66 g, 8.86 mmol). The reaction mixture was heated at 80 °C overnight. The reaction mixture was concentrated in vacuo. The resulting residue was purified by silica gel chromatography (1−15% MeOH/CH_2Cl_2 gradient) to afford 1.48 g (58%) of the desired product: LCMS t_R = 2.05 min, (M + H) 576.47.

(*R*)-3-((*S*)-3-((2-(5-Chloro-1*H*-pyrrolo[2,3-*b*]pyridin-3-yl)-5-fluoropyrimidin-4-yl)amino)piperidin-1-yl)propane-1,2-diol (10). To a solution of (*R*)-3-((*S*)-3-((2-(5-chloro-1-tosyl-1*H*-pyrrolo-[2,3-*b*]pyridin-3-yl)-5-fluoropyrimidin-4-yl)amino)piperidin-1-yl)-propane-1,2-diol, **17b** (1.48 g, 2.57 mmol), in methanol (20 mL) was added sodium methoxide (10 mL of 25% w/v solution, 46.28 mmol). After 5 min, the reaction mixture was diluted into water and extracted twice with EtOAc. The combined organic phases were dried ($MgSO_4$), filtered, and concentrated in vacuo. The resulting residue was purified by silica gel chromatography (1−20% MeOH/CH_2Cl_2 gradient) to afford 0.66 g (45%) of the desired product: ^{1}H NMR (300 MHz, DMSO-d_6) δ 12.31 (s, 1H), 8.72 (d, J = 2.4 Hz, 1H), 8.28 (d, J = 2.4 Hz, 1H), 8.20 (s, 1H), 8.17 (d, J = 4.0 Hz, 1H), 7.33 (d, J = 7.6 Hz, 1H), 4.51 (m, 1H), 4.37 (s, 1H), 4.25 (m, 1H), 3.64 (m, 1H), 3.35 (s, 2H), 3.08−2.95 (m, 1H), 2.80−2.70 (m, 1H), 2.47−2.25 (m, 2H), 2.22−2.12 (m, 2H), 1.99−1.90 (m, 1H), 1.70−1.60 (m, 2H), and 1.45 (m, 1H) ppm; HRMS (ESI) of $C_{19}H_{23}ClFN_6O_2$ [M + H] calcd, 421.154 95; found, 421.154 54.

***meso-endo*-Tetrahydro-4,7-ethanoisobenzofuran-1,3-dione (50).** To a cold (0 °C) solution of maleic anhydride (210.0 g, 2142.0 mmol) in $CHCl_3$ (2.3 L) was added cyclohexa-1,3-diene (224.5 mL, 2356.0 mmol) slowly over 50 min. The mixture was warmed to room temperature and stirred overnight in the dark. After removal of the solvent under reduced pressure, 2.1 L of MeOH was added to the mixture and the mixture was heated to 50 °C for 10 min and then cooled to 0 °C. The resulting precipitate was filtered and dried in an oven at 45 °C overnight to afford 283 g of a white solid. The resulting *endo* (*meso*) Diels−Alder cycloaddition product was used without further purification.

(±)-*trans*-3-(Methoxycarbonyl)bicyclo[2.2.2]oct-5-ene-2-carboxylic Acid (51). A solution of *meso-endo*-tetrahydro-4,7-ethanoisobenzofuran-1,3-dione, **50** (74.5 g, 418.1 mmol), was stirred in NaOMe (764.9 mL of 25% w/w solution in MeOH, 3345.0 mmol). The reaction mixture was stirred at room temperature for 4 days, yielding a white suspension. The reaction mixture was concentrated in vacuo to remove approximately 300 mL of MeOH. In another flask, HCl (315.9 mL of 36.5% w/w, 3763.0 mmol) in 300 mL of water was cooled to 0 °C. The reaction mixture was added into this HCl solution slowly, and a white solid precipitated. The remaining methanol was removed under reduced pressure. The mixture was cooled to 0 °C and stirred for 30 min. The precipitate was filtered, washed with water 3 times, giving an off-white solid. The remaining water was removed under reduced pressure to afford 82 g of a white solid that was used without further purification.

(±)-*trans*-Methyl 3-(((Benzyloxy)carbonyl)amino)-bicyclo[2.2.2]oct-5-ene-2-carboxylate (52). Racemic *trans*-3-methoxycarbonylbicyclo[2.2.2]oct-5-ene-2-carboxylic acid, **51** (100.0 g, 475.7 mmol), was dissolved in toluene (1.0 L). Diphenylphosphorylazide (112.8 mL, 523.3 mmol) and triethylamine (72.9 mL, 523.3 mmol) were added. The reaction mixture was heated to 90 °C for 2 h. Benzyl alcohol (49.2 mL, 475.7 mmol) was added, and the mixture was heated to 90 °C over 3 days. The mixture was cooled to room temperature and diluted with EtOAc (500 mL) and aqueous saturated $NaHCO_3$ solution. The organic phase was washed with brine, dried ($MgSO_4$), filtered, and concentrated in vacuo. The resulting crude material was purified by silica gel chromatography with dichloromethane to afford 115 g of oil (77%). ^{1}H NMR show it contains BnOH (about 0.05 equiv). Product was used without further purification: ^{1}H NMR (300 MHz, $CDCl_3$) δ 7.40−7.24 (m, 5H), 6.41 (t, J = 7.4 Hz, 1H), 6.21−6.04 (m, 1H), 5.15−4.94 (m, 2H), 4.63−4.45 (m, 1H), 4.30−4.18 (m, 1H), 3.70 (s, 2H), 3.49 (s, 1H), 2.81 (br s, 1H), 2.68 (br s, 1H), 2.08 (s, 1H), 1.76−1.56 (m, 1H), 1.52−1.35 (m, 1H), 1.33−1.14 (m, 1H), 1.12−0.87 (m, 1H) ppm.

(±)-*trans*-Methyl 3-Aminobicyclo[2.2.2]octane-2-carboxylate (53). A solution of racemic *trans*-methyl 3-(((benzyloxy)-carbonyl)amino)bicyclo[2.2.2]oct-5-ene-2-carboxylate, **52** (115.0 g, 364.7 mmol), in THF (253 mL) and MeOH (253 mL) was placed under 40 psi of hydrogen overnight. Some exotherm was observed. The reaction mixture was filtered through Celite and washed with MeOH. The filtrate was concentrated in vacuo to afford 69 g of the desired product as an oil: ^{1}H NMR (400 MHz, $CDCl_3$) δ 3.63 (d, J = 5.6 Hz, 3H), 3.30 (d, J = 6.7 Hz, 1H), 2.11 (d, J = 6.6 Hz, 1H), 1.91 (t, J = 7.3 Hz, 1H), 1.80−1.64 (m, 1H), 1.63−1.38 (m, 6H), 1.36−1.23 (m, 2H) ppm.

(2*S*,3*S*)-Methyl 3-((2-Chloro-5-fluoropyrimidin-4-yl)amino)-bicyclo-[2.2.2]octane-2-carboxylate (55). To a solution of racemic-*trans*-methyl 3-aminobicyclo[2.2.2]octane-2-carboxylate, **53** (1.30 g, 7.09 mmol), and 2,4-dichloro-5-fluoropyrimidine (1.77 g, 10.64 mmol) in DMF (20 mL) was added *N*,*N*-diisopropylethylamine (4.94 mL, 28.38 mmol). The reaction mixture was stirred at room temperature for 100 min. The mixture was diluted into aqueous saturated NH_4Cl solution and extracted twice with EtOAc. The combined organic phases were washed three times with brine, dried ($MgSO_4$), filtered, and concentrated in vacuo. The crude residue was purified via silica gel chromatography (0−10% MeOH/CH_2Cl_2 gradient) to afford 1.41 g of the racemic product, **39**: LC/MS gradient 10−90%, 0.1% formic acid, 5 min, C18/ACN t_R = 1.14 min, (M + H) 314.11.

The racemic product **54** was submitted for SFC chiral separation to afford the single enantiomer **55**.

(2*S*,3*S*)-Methyl 3-((5-Fluoro-2-(5-fluoro-1-tosyl-1*H*-pyrrolo-[2,3-*b*]pyridin-3-yl)pyrimidin-4-yl)amino)bicyclo[2.2.2]octane-2-carboxylate (57). A mixture of 5-fluoro-1-(*p*-tolylsulfonyl)-3-(4,4,5,5-tetramethyl-1,3,2-dioxaborolan-2-yl)pyrrolo[2,3-*b*]pyridine, **56** (10.22 g, 24.54 mmol), (2*S*,3*S*)-methyl 3-((2-chloro-5-fluoropyrimidin-4-yl)amino)bicyclo[2.2.2]octane-2-carboxylate, **55**, (5.5 g, 17.53 mmol), K_3PO_4 (0.95 g, 2.92 mmol) in 2-methyl THF (100 mL), and H_2O (20 mL) was degassed under a stream of nitrogen for 15 min. To the mixture was added X-Phos (1.00 g, 2.10 mmol) and 1,5-diphenylpenta-1,4-dien-3-one, palladium (0.40 g, 0.44 mmol). The reaction vessel was sealed and heated to 115 °C for 3 h. The aqueous phase was removed, and the organic phase was filtered through Celite and concentrated in vacuo. The resulting residue was purified by silica gel chromatography (20% EtOAc/hexanes) to afford 9.5 g (95%) of the desired product: LCMS gradient 10−90%, 0.1% formic acid, 5 min, C18/ACN, t_R = 4.2 min, (M + H) 567.84.

(2*S*,3*S*)-Methyl 3-((5-Fluoro-2-(5-fluoro-1*H*-pyrrolo[2,3-*b*]-pyridin-3-yl)pyrimidin-4-yl)amino)bicyclo[2.2.2]octane-2-carboxylate (58). To a mixture of (2*S*,3*S*)-methyl 3-((5-fluoro-2-(5-fluoro-1-tosyl-1*H*-pyrrolo[2,3-*b*]pyridin-3-yl)pyrimidin-4-yl)amino)-bicyclo[2.2.2]octane-2-carboxylate, **57** (7.44 g, 13.11 mmol), in CH_3CN (40 mL) at room temperature was added HCl (19.66 mL of 4 M solution in dioxane, 78.66 mmol). The resulting solution was heated to 65−70 °C for 6.5 h and then cooled to room temperature where stirring was maintained overnight. The mixture was diluted with MTBE, and the resulting precipitate was filtered. The solid was suspended in MBTE and filtered twice more. The solid was dried

dx.doi.org/10.1021/jm5007275 | J. Med. Chem. 2014, 57, 6668−6678

under vacuum to afford 6.36 g (95%) of the desired product as the hydrochloride salt: ^{1}H NMR (400 MHz, MeOD) δ 8.57 (dd, J = 9.1, 2.7 Hz, 1H), 8.50 (s, 1H), 8.35 (s, 1H), 8.31 (d, J = 5.6 Hz, 1H), 5.18 (d, J = 6.5 Hz, 1H), 3.70 (s, 3H), 2.97 (d, J = 6.7 Hz, 1H), 2.15 (s, 1H), 2.05 (s, 1H), 2.01−1.50 (m, 8H).

(2*S*,3*S*)-3-((5-Fluoro-2-(5-fluoro-1*H*-pyrrolo[2,3-*b*]pyridin-3-yl)pyrimidin-4-yl)amino)bicyclo[2.2.2]octane-2-carboxylic Acid (2). A solution of NaOH (119.5 mL of 2 N solution, 239.0 mmol) was added to a solution of (2*S*,3*S*)-methyl 3-((5-fluoro-2-(5-fluoro-1*H*-pyrrolo[2,3-*b*]pyridin-3-yl)pyrimidin-4-yl)amino)bicyclo-[2.2.2]octane-2-carboxylate, **58** (24.7 g, 59.8 mmol), in methanol (98 mL) and THF (98 mL). The reaction mixture was stirred at 30 °C for 2 h. The mixture was cooled to room temperature and stirred overnight. The organic solvents were concentrated under vacuum. 2-Methyl THF was added (150 mL), and the organics were concentrated in vacuo. Additional 2-methyl THF was added, and the mixture was neutralized with 6 N HCl while stirring the biphasic mixture vigorously. The organic layer was separated, and the aqueous layer was extracted with 2-methyl THF (3 × 200 mL), adjusting the pH between each extraction to ∼pH 6. The combined organic phases were dried over Na_2SO_4, filtered, and concentrated in vacuo. The solid was taken up again in a large volume of warm 2-methyl THF and filtered again through Celite. The clear solution was concentrated in vacuo and dried in a vacuum oven overnight at 50 °C, followed by an additional night at 80−85 °C to afford 22.75 g of the desired product: ^{1}H NMR (300 MHz, DMSO-d_6) δ 12.71 (br s, 1H), 8.58 (s, 1H), 8.47 (dd, J = 9.6, 2.8 Hz, 1H), 8.41 (d, J = 4.8 Hz, 1H), 8.39−8.34 (m, 1H), 4.89−4.76 (m, 1H), 2.94 (d, J = 6.9 Hz, 1H), 2.05 (br s, 1H), 1.96 (br s, 1H), 1.68 (complex m, 7H); ^{13}C NMR (300 MHz, DMSO-d_6) δ 174.96, 157.00, 155.07, 153.34, 152.97, 145.61, 142.67, 140.65, 134.24, 133.00, 118.02, 114.71, 51.62, 46.73, 28.44, 28.00, 24.90, 23.78, 20.88, 18.98; LCMS gradient 10−90%, 0.1% formic acid, 5 min, C18/ACN, t_R = 2.24 min, (M + H) 400.14; HRMS (ESI) of $C_{20}H_{20}F_2N_5O_2$ [M + H] calcd, 400.157 95; found, 400.157 56.

In Vitro Antiviral Assays. Details are presented in the Supporting Information. MDCK cell protection and cytotoxicity assays were performed using a modification of standard methods, essentially the 3-day CPE-based approach employing an ATP cell viability end point. Replication of influenza virus RNA, either positive-strand or negative-strand polarity, was measured using strand-specific probes using the bDNA QuantiGene method (Affymetrix), as previously described. Influenza virus sensitivity to the neuraminidase inhibitors oseltamivir carboxylate and zanamivir was determined by the chemiluminescent neuraminidase inhibitor assay using the NA-XTD kit (Applied Biosystems; Foster City, CA) per the manufacturer's recommendations.

■ ASSOCIATED CONTENT

Ⓢ Supporting Information

^{1}H NMR, MS, and HRMS spectral data for all of the final compounds; experimental details for **7**, **9**−**11**, **18**, **20**, **21**, **26**, **28**, **29**, **31**, **40**, **42**, **45**, and **46**; protocols for PB2 binding assay; CPE and bDNA cellular assays; mouse influenza pharmacology models. This material is available free of charge via the Internet at http://pubs.acs.org.

■ AUTHOR INFORMATION

Corresponding Author

*Phone: 617-961-7727. E-mail: michael_clark@vrtx.com.

Author Contributions

The manuscript was written through contributions of all authors. All authors have given approval to the final version of the manuscript.

Notes

The authors declare no competing financial interest.

■ ACKNOWLEDGMENTS

We thank Barry Davis, Nigel Ewing, and Ravikanth Veluri for high-resolution mass spectrometric determination of key compounds. We thank Brian Krueger for invaluable SFC chiral purifications. In addition, we thank Yuegang Zhang for small molecule X-ray crystallography.

■ ABBREVIATIONS USED

bDNA, branched DNA; SAR, structure−activity relationship; AUC, area under curve; CPE, cytopathic effect assay; b.i.d., twice a day dosing; SOC, standard of care; m^{7}GTP, methyl-7-guanosine 5′-triphosphate; $NaHCO_3$, sodium bicarbonate; EtOH, ethanol; ^{i}Pr$_2$NEt, diisopropylethyl amine; NaOMe, sodium methoxide; KOAc, potassium acetate; $PdCl_2$(dppf), [1,1′-bis(diphenylphosphino)ferrocene]dichloropalladium(II), complex with dichloromethane; $Pd(PPh_3)_4$, tetrakis-(triphenylphosphine)palladium(0); DPPA, diphenylphosphoryl azide; BnOH, benzyl alcohol; C_{max}, maximum concentration that a drug achieves after dosing; C_{min}, minimum concentration that a drug achieves after dosing and prior to following dose; $TCID_{50}$, 50% tissue culture infective dose

■ REFERENCES

(1) Wagaman, P. C.; Leong, M. A.; Simmen, K. A. Development of a novel influenza A antiviral assay. *J. Virol. Methods* **2002**, *105*, 105−114.

(2) Thompson, W. W.; Shay, D. K.; Weintraub, E.; Brammer, L.; Bridges, C. B.; Cox, N. J.; Fukuda, K. Influenza-associated hospitalizations in the United States. *JAMA, J. Am. Med. Assoc.* **2004**, *292*, 1333−1340.

(3) CDC. Seasonal Influenza: Key Facts about Influenza (Flu) and Flu Vaccine. http://cdc.gov/flu/keyfacts.htm (accessed July 30, 2012).

(4) (a) Cohen, J. Surprising twist in debate over lab-made H5N1. *Science* **2012**, *335*, 1155−1156. (b) Herfst, S.; Schrauwen, J. A.; Linster, M.; Chutinimitkul, S.; deWit, E.; Munster, V. J.; Sorrell, E. M.; Bestebroer, T. M.; Burke, D. F.; Smith, D. J.; Rimmelzwaan, G. F.; Osterhaus, A. D. M. E.; Fouchier, R. A. M. Airborne transmission of influenza A/H5N1 virus between ferrets. *Science* **2012**, *336*, 1524−1541.

(5) Moscona, A. Neuraminidase inhibitors for influenza. *N. Engl. J. Med.* **2005**, *353*, 1363−1373.

(6) Thorland, K.; Awad, T.; Boivin, G.; Thabane, L. Systematic review of influenza resistance to the neuraminidase inhibitors. *BMC Infect. Dis.* **2011**, *11*, 134.

(7) Le, Q. M.; Kiso, M.; Someya, K.; Sakai, Y. T.; Nguyen, T. H.; Nguyen, K. H. L.; Pham, N. D.; Ngyn, H. H.; Yamada, S.; Muramoto, Y.; Horimoto, T.; Takada, A.; Goto, H.; Suzuki, Y.; Kawaoka, Y. Avian flu: isolation of drug-resistant H5N1 virus. *Nature* **2005**, *437*, 1108.

(8) Noah, J. W.; Severson, W.; Noah, D. L.; Rasmussen, L.; White, E. L.; Jonsson, C. B. A cell-based luminescence assay is effective for high-throughput screening of potential influenza antivirals. *Antiviral Res.* **2007**, *73*, 50−59.

(9) (a) Guilligay, D.; Tarendeau, F.; Resa-Infante, P.; Coloma, R.; Crepin, T.; Sehr, P.; Lewis, J.; Ruigrok, R. W.; Ortin, J.; Hart, D. J.; Cusack, S. The structural basis for cap binding by influenza virus polymerase subunit PB2. *Nat. Struct. Mol. Biol.* **2008**, *15*, 500−506. (b) Pautus, S.; Sehr, P.; Lewis, J.; Fortune, A.; Wolkerstorfer, A.; Szolar, O.; Guilligay, D.; Lundardi, T.; Decout, J.-L.; Cusack, S. New 7-methylguanine derivatives targeting the influenza polymerase PB2 cap-binding domain. *J. Med. Chem.* **2013**, *56*, 8915−8930.

(10) Fechter, P.; Mingay, L.; Sharps, J.; Chambers, A.; Fodor, E.; Brownlee, G. G. Two aromatic residues in the PB2 subunit of influenza A RNA polymerase are crucial for cap binding. *J. Biol. Chem.* **2003**, *278*, 20381−20388.

(11) Palese, P.; Shaw, M. L. Orthomyxoviridae: The Viruses and Their Replication. In *Fields Virology*; Knipe, D. M., Howley, P. M.,

Eds.; Lippincott Williams & Wilkins: Philadelphia, PA, 2007; pp 1647−1689.
(12) Charifson, P. S.; Clark, M. P.; Bandarage, U. K.; Bethiel, R. S.; Boyd, M. J.; Davies, I.; Deng, H.; Duffy, J. P.; Farmer, L. J.; Gao, H.; Gu, W.; Kennedy, J. M.; Ledford, B.; Ledeboer, M. W.; Maltais, F.; Perola, E.; Wang, T. Inhibitors of Influenza Viruses Replication. WO 2013/019828, February 2, 2013.
(13) Byrn, R. A.; Jones, S.; Asmal, M.; Bennett, H. B.; Bral, C.; Clark, M. P.; Jacobs, M.; Kwong, A.; Ledeboer, M.; Leeman, J. R.; McNeil, C.; Murcko, M.; Nezami, A.; Perola, E.; Rijnbrand, R.; Saxena, K.; Travejo, J.; Tsai, A.; Zhou, Y.; Charifson, P. S.; Preclinical activity of VX-787, a first-in-class, orally bioavailable inhibitor of the influenza viral polymerase PB2 subunit. Manuscript submitted for publication.
(14) Memmott, C.; Taylor, W. Manuscript in preparation.
(15) Kerns, E.; Di, L. Transporters. In *Drug-like Properties: Concepts, Structure, Design and Methods*; Elsevier: Burlington, MA, 2008; pp 103−121.